JOURNAL OF GUIDANCE, CONTROL, AND DYNAMICS
Vol. 19, No. 4, July–August 1996

# Motion Control of Free-Floating Variable Geometry Truss Part 2: Inverse Kinematics

Shengyang Huang
*Toyota Technological Institute, Tempaku, Nagoya 468, Japan*
M. C. Natori
*Institute of Space and Astronautical Science, Sagamihara 229, Japan*
and
Kohichi Miura
*Nihon University, Narashinodai, Funabashi 274, Japan*

**The inverse kinematics of a free-floating variable geometry truss are formulated in conjunction with the conservation of momentum, and the Moore–Penrose inverse is employed to give the solution. Based on the generalized Jacobian matrix, a two-order solution of task priority is derived, and its possible applications to obstacle avoidance, shape control, and free-endplane control are also discussed. Moreover, the issues of the dynamic singularities of a free-floating variable geometry truss are addressed, and an approach through actively handling the orientation of the free-endplane of a free-floating variable geometry truss is proposed to reduce the coupling of singularities with its dynamic parameters. With the aim of applications in space engineering, a free-floating variable geometry truss model is manufactured and set up in the laboratory, and a distributed control architecture is constructed to provide it with an effective parallel control. Finally, a docking experiment with this model is carried out.**

---

**Shenyang Huang received his B.Eng. degree in applied machanics from Huazhong University of Science and Technology, China, in 1983 and the M.Eng. and Ph.D. degrees, both in computational mechanics, from Dalian University of Technology, China, in 1983 and 1989, respectively. In 1990, he joined the Dalian University of Technology as a lecturer. From January 1991 to June 1994, he was a foreign research fellow in spacecraft engineering at the Institute of Space and Astronautical Science, Japan. Since July 1994, he has been an invited research fellow at the Intelligent System Laboratory of the Toyota Technological Institute, Japan. His research interests include engineering database systems, knowledge-based systems, object-oriented approaches, distributed autonomous systems, and motion controls of intelligent adaptive structures.**

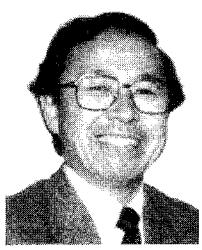

**M. C. Natori received his B.S., M.S., and D.Eng. degrees from the University of Tokyo, Japan, in 1967, 1969, and 1972, respectively. He worked at the Institute of Space and Aeronautical Science of the University of Tokyo and joined the faculty of the Institute of Space and Astronautical Science in 1983. Currently, he is a professor of spacecraft engineering at the Institute of Space and Astronautical Science and also at the University of Tokyo. His major research fields are space structures engineering, structural dynamics and control, aeroelasticity, and science on form. Dr. Natori is currently an experiments manager of the Space Flyer Unit, a manager of the MUSES-B antenna structure development for the Japanese space VLBI program, and a cochair of the Department of Architecture at the International Space University. He is a member of the Structures Technical Committee of the AIAA, the Adaptive Structures Technical Committee of the American Society of Mechanical Engineers, the Japan Society for Aeronautical and Space Sciences, the Japan Society of Mechanical Engineers, and the Society of Science on Form (Editorial Board). He is also a member of the editorial board of two journals: *Smart Materials and Structures* and *Journal of Intelligent Material Systems and Structures*.**

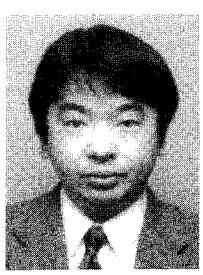

**Kohichi Miura received his B.Eng. and M.Eng. degrees, both in mechanical engineering, from Nihon University, Japan, in 1980 and 1982, respectively. Since 1985, he has been a research associate at the Department of Junior College, Nihon University. His research interests include dynamics and control of intelligent adaptive structures.**

Received April 20, 1994; revision received Feb. 19, 1996; accepted for publication Feb. 26, 1996. 

## I. Introduction

THE performance required for future space structures has motivated the concept of adaptive structures, among which the most widely investigated is a variable geometry truss (VGT). A VGT usually has a large variety of length-adjustable actuators as its members and is very stiff. Several applications of it, such as large space robots, etc., in space engineering, have been proposed in recent investigations. However, these applications all make use of VGT's ability to change its geometry to develop large workable machines, that is, they fall into the same category where the motion feature is kinematic and VGTs are fixed to some base platforms with one endplane. In Part 1 of this study, the authors suggest an alternate application for VGTs, where VGTs are utilized as intelligent structures that (except for their major structural functions) possess some workable abilities to assemble themselves to form some larger space structures.[1] The basic feature of VGTs in this case is that they are free floating, and their fundamental kinematics have been dealt with in detail and presented in Part 1 of this investigation. For VGTs to autonomously assemble, the most basic working task for VGTs is to overcome the docking problem in the free-floating state, for which the inverse kinematic control is widely applied. In the case of a free-floating VGT, it is not enough to determine its motion only with kinematics. Therefore, the conservation of momentum of a system was proposed to establish the dynamics for a free-floating manipulator.[2] Using the so-called generalized Jacobian matrix, the motion governing equations of a free-floating manipulator can be built up in a way similar to those used to define movement of manipulators with fixed-bases. However, the generalized Jacobian matrix would couple its dynamic properties with the singular configurations of a free-floating VGT, bringing about difficulties in determining its singularities. This can be a serious problem in maneuvering a VGT. Because a VGT is commonly highly redundant, how to construct a control architecture for it is a key issue to effectively achieve its real-time control.

This paper presents the successive progress of the investigation reported in Part 1, which deals with the inverse kinematics of a free-floating VGT and describes a docking experiment. First, the inverse kinematics of free-floating VGTs for a docking control are formulated. Then the simple Moore–Penrose inverse is used to solve the inverse kinematics. Regarding the high redundancy of a VGT, a two-order solution of task priority is derived from the generalized Jacobian matrix, whose results might indicate several applications such as obstacle avoidance, shape control, free-endplane control, and so on. Concerning the dynamic singularities, instead of the generalized Jacobian matrix, it is proposed that a pseudokinematic Jacobian matrix can be used to reduce the dynamic dependence of the singularities of a free-floating VGT if its free-endplane is actively controlled. To effectively control a VGT, a distributed control architecture is built in the laboratory, which is used to carry out a docking experiment.

## II. Structural Model and Kinematics Governing Equations

This study is carried out using the basic assumptions adopted in Part 1, where a free-floating VGT, as a dynamic conservative system, is taken into account in three-dimensional null-gravity space. Also, a VGT is assumed to move so slowly that its structural vibration can be neglected. A VGT consists of $N$ bays in total, each bay of which is a truss comprising 3 identical equilateral triangular truss battens and 12 diagonal members (see Part 1). These bays are joined by sharing a common lateral triangular truss that corresponds to the top and bottom plane of two adjacent bays, respectively (Fig. 1). The kinematics model of the structure is established on the fundamental abstraction of a so-called logic bay that is similar in geometric configuration to a VGT bay with the exception that the bottom plane of a logic bay only virtually exists, and there is a virtual bay that is defined in response to the free endplane of the structure. The shape curve formed by the structure can be determined with the center of mass vector of a passive plane, which corresponds to either the bottom or the top plane of a bay and is not actuator equipped.

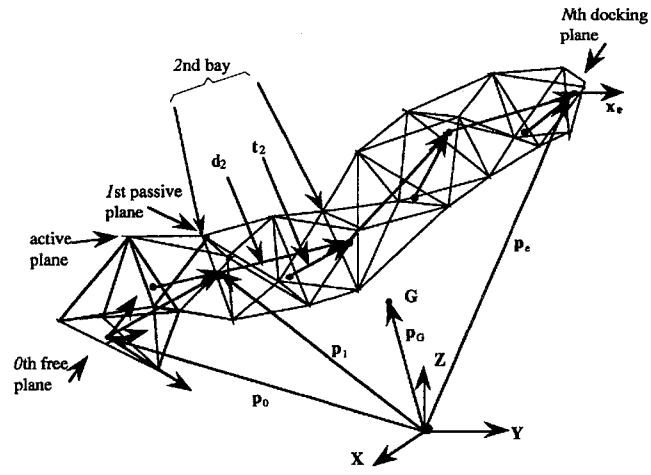


**Fig. 1 Chain model of a free-floating VGT.**

When the motion control of a free-floating VGT is dealt with, the velocity governing equation for a passive plane, which has been presented in Part 1, is of key importance and takes the form

$$\dot{\boldsymbol{p}}_i = \boldsymbol{A}_{i,0}\dot{\boldsymbol{\Phi}}_0 + \sum_{k=1}^{N} \boldsymbol{A}_{i,k}\dot{\boldsymbol{d}}_k \qquad (i = 0, \ldots, N) \tag{1}$$

where $\boldsymbol{p}_i$ is the center of mass vector of the $i$th passive plane; $\boldsymbol{A}_{i,0}$ is the contribution matrix to the center velocity of mass of the $i$th plane from the free endplane, namely, the 0th passive plane; $\boldsymbol{\Phi}_0$ is the vector depicting the attitude of the free endplane; and $\boldsymbol{d}_k$ is the governing vector of the $k$th bay, which stretches between the bottom and top plane of the bay and is defined with respect to the bay relative reference frame.

As to the orientation control of a passive plane, we also have the following control equation for its angular velocity:

$$\boldsymbol{\omega}_i = \boldsymbol{P}_0\dot{\boldsymbol{\Phi}}_0 + \sum_{j=1}^{i} {}^{A}\boldsymbol{P}_j\dot{\boldsymbol{d}}_j \qquad (i = 0, \ldots, N) \tag{2}$$

where $\boldsymbol{\omega}_i$ is the angular velocity of an arbitrary passive plane of the structure, which is described in the inertial reference frame, and ${}^{A}\boldsymbol{P}_j$ is a mapping matrix.

Concerning the dynamics of a free-floating VGT, we can establish the following relationship according to the conservation of angular momentum of the system:

$$\boldsymbol{H}_0\dot{\boldsymbol{\Phi}}_0 + \sum_{i=1}^{N} \boldsymbol{H}_i\dot{\boldsymbol{d}}_i = \text{const} \tag{3}$$

where $\boldsymbol{H}_i$ is the contribution matrix of the $i$th bay to the total angular momentum of structure.

If a structure is assumed initially static, then const becomes zero, such that $\boldsymbol{\Phi}_0$ can be solved explicitly as

$$\dot{\boldsymbol{\Phi}}_0 = -\sum_{i=1}^{N} \boldsymbol{H}_0^{-1}\boldsymbol{H}_i\dot{\boldsymbol{d}}_i \tag{4}$$

Equations (1) and (2) along with Eq. (3) or (4) provide the fundamental kinematics for a free-floating VGT.

## III. Inverse Kinematics of a Free-Floating VGT

### A. Resolved Motion Rate Control

The inverse kinematics control for robotic manipulators is commonly characterized by the direct maneuvering of their end-effectors through prespecified trajectories. Concerning a free-floating VGT, we can take one of its endplanes as the end effector to establish the inverse kinematics in a way similar to manipulators. Without loss of generality, we take the $N$th passive plane to be the docking plane. The center of mass velocity is given by Eq. (1) and the angular velocity by Eq. (2). With Eq. (3), we can eliminate the coupling

effect on the docking plane resulting from the rotation of the free endplane

$$\dot{\boldsymbol{p}}_N = \sum_{k=1}^{N} \left(\boldsymbol{A}_{N,k} - \boldsymbol{A}_{N,0}\boldsymbol{H}_0^{-1}\boldsymbol{H}_k\right)\dot{\boldsymbol{d}}_k \tag{5}$$

Similarly,

$$\omega_N = \sum_{k=1}^{N} \left({}^{A}\boldsymbol{P}_j - \boldsymbol{P}_0\boldsymbol{H}_0^{-1}\boldsymbol{H}_k\right)\dot{\boldsymbol{d}}_k \tag{6}$$

Usually, structural singularities occur while all rotational variables of the docking plane are taken into account. Consequently, some rotational degrees of freedom (DOF) can be taken away to serve other tasks such as the optimization of structural configuration. A proposed selection for the control vector is the differentiation of the normal vector of the docking plane. It is known that the normal vector of the docking plane $\boldsymbol{n}_e$ is given by

$$\boldsymbol{n}_e = {}^{A}\boldsymbol{D}_e\boldsymbol{n}$$

where $\boldsymbol{n}$ is another representation of $\boldsymbol{n}_e$ and is defined in a reference frame that is located at the docking plane. ${}^{A}\boldsymbol{D}_e$ is the transformation matrix of the docking plane with respect to the inertial reference frame.

By differentiating $\boldsymbol{n}_e$, we can obtain

$$\frac{\mathrm{d}\boldsymbol{n}_e}{\mathrm{d}t} = \omega_N \times \boldsymbol{n}_e$$

Upon substitution of Eq. (6), we arrive at

$$\frac{\mathrm{d}\boldsymbol{n}_e}{\mathrm{d}t} = \sum_{k=1}^{N} \left(\boldsymbol{N}_k - \boldsymbol{N}_0\boldsymbol{H}_0^{-1}\boldsymbol{H}_k\right)\dot{\boldsymbol{d}}_k \tag{7}$$

$$\boldsymbol{N}_k = -\tilde{\boldsymbol{n}}_e\,{}^{A}\boldsymbol{P}_k \tag{7a}$$

where $\tilde{\boldsymbol{n}}_e$ is the skew matrix of vector $\boldsymbol{n}_e$.

Assuming the particular control variables for the free endplane is $\Phi = \{\alpha, \beta, \ldots\}$ and the transformation matrix between $\boldsymbol{n}_e$ and $\Phi$ is $\bar{\Phi}$, then after combining Eqs. (5) and (6), we can establish the control scheme of resolved motion rate control[3]

$$\dot{\boldsymbol{x}}_e = \boldsymbol{J}_e\dot{\boldsymbol{d}} \tag{8}$$

where $\dot{\boldsymbol{d}} = \{\dot{\boldsymbol{d}}_1, \ldots, \dot{\boldsymbol{d}}_N\}$, $\dot{\boldsymbol{x}}_e$ is the control vector of the docking plane, and $\boldsymbol{J}_G$ is the Jacobian matrix, which is represented by

$$\boldsymbol{J}_e = \{\boldsymbol{J}_t, \boldsymbol{J}_r\}^T \tag{8a}$$

$$\boldsymbol{J}_t = \left\{-\boldsymbol{A}_{N,0}\boldsymbol{H}_0^{-1}\boldsymbol{H}_1 + \boldsymbol{A}_{N,1}, \ldots, -\boldsymbol{A}_{N,0}\boldsymbol{H}_0^{-1}\boldsymbol{H}_N + \boldsymbol{A}_{N,N}\right\} \tag{8b}$$

$$\boldsymbol{J}_r = \left\{\bar{\Phi}\left(-\boldsymbol{N}_0\boldsymbol{H}_0^{-1}\boldsymbol{H}_1 + \boldsymbol{N}_1\right), \ldots, \bar{\Phi}\left(-\boldsymbol{N}_0\boldsymbol{H}_0^{-1}\boldsymbol{H}_N + \boldsymbol{N}_N\right)\right\} \tag{8c}$$

### B. Solution Analysis of Inverse Kinematics

If the DOF of the docking control vector is exactly equal to the number of actuators a VGT is equipped with, then the inverse kinematics solution can be easily discovered by solving a group of linear equations. However, the case most commonly encountered for Eq. (8) is a underdetermined equation group resulting from the high redundancy of the DOF of a VGT structure. In fact, the high redundancy of a VGT makes a series of tasks possible, including the ability to simultaneously govern the two endplanes of the structure, avoid obstacles and singular states where the structures would lose some DOF, keep away from the motion limits of variable members, and so on. To make full use of these abilities, effective control algorithms must be developed, to which end we focus primarily on the relatively simple Moore–Penrose theory, which is applied broadly in the control of robotic manipulators.

A general formulation in terms of Moore–Penrose inverse was suggested by Liegeois,[4] which takes the form

$$\dot{\boldsymbol{d}} = \boldsymbol{J}_e^{+}\dot{\boldsymbol{x}}_e + \left(\boldsymbol{I} - \boldsymbol{J}_e^{+}\boldsymbol{J}_e\right)\dot{\boldsymbol{d}}_r' \tag{9}$$

where

$$\boldsymbol{J}_e^{+} = \boldsymbol{J}_e^T\left(\boldsymbol{J}_e\boldsymbol{J}_e^T\right)^{-1} \tag{9d}$$

is the so-called Moore–Penrose inverse, $\dot{\boldsymbol{d}}_r'$ is an arbitrary vector that is added to the solution for some other tasks, and matrix $(\boldsymbol{I} - \boldsymbol{J}_e^{+}\boldsymbol{J}_e)$ is a projectional operator, which is orthogonal to $\boldsymbol{J}_e$ and projects vector $\dot{\boldsymbol{d}}_r'$ onto the null space of $\boldsymbol{J}_e$. Hence, the vector $(\boldsymbol{I} - \boldsymbol{J}_e^{+}\boldsymbol{J}_e)\dot{\boldsymbol{d}}_r'$ stands for the general solution of the homogeneous equation $\boldsymbol{J}_e\dot{\boldsymbol{d}}_r' = 0$. We call the vector space projected by the operator $(\boldsymbol{I} - \boldsymbol{J}_e^{+}\boldsymbol{J}_e)$ the null space of $\boldsymbol{J}_e$, and express it as $N(\boldsymbol{J}_e)$.

#### 1. *Dimensional Inhomogeneity of the Inverse Kinematic Solution*

In general, for a singular linear system $\boldsymbol{x} = \boldsymbol{A}\boldsymbol{u}$, the Moore–Penrose inverse can be employed to produce a least-squares and minimum-norm solution to it, as long as the vector space $U$ of vector $\boldsymbol{u}$ and the vector space $X$ of vector $\boldsymbol{x}$ are Euclidean-normed spaces. However, as Doty et al.[5] pointed out, arbitrary assignment of Euclidean inner products to the space $U$ and $X$, when the vector $\boldsymbol{u}$ and $\boldsymbol{x}$ have elements with different physical units, can lead to inconsistent and noninvariant results. These results can be obtained when the reference frame and/or unit of elements for the vector $\boldsymbol{u}$ and $\boldsymbol{x}$ get changed. In our case, the end-effector vector $\boldsymbol{x}_e$ consists of both the center of mass velocity and the angular velocity of the end effector, so that there is no physically consistent Euclidean inner products for it. Therefore, whether the simple Moore–Penrose inverse can be still used in our case becomes a problem, which is briefly discussed using the theory of Doty et al.[5] Because vector $\dot{\boldsymbol{d}}$ in the vector space $U$ is physically consistent, just the vector $\dot{\boldsymbol{x}}_e$ of the vector space $X$ needs to be taken into account.

Concerning the physically inconsistent vector $\dot{\boldsymbol{x}}_e$, a generalized inner product can be defined in place of the Euclidean inner products. Select a positive definite symmetric matrix $\boldsymbol{M}_x$ such that the inner product

$$\dot{\boldsymbol{x}}_e^T\boldsymbol{M}_x\dot{\boldsymbol{x}}_e = \sum_{i=1}^{m}\sum_{j=1}^{m} m_{xi,j}\dot{x}_{ei}\dot{x}_{ei} \tag{10}$$

will make sense in terms of physical units. If matrix $\boldsymbol{J}_e$ has a full-rank decomposition[6] $\boldsymbol{J}_e = \boldsymbol{F}\boldsymbol{C}$ that satisfies

$$\text{rank}[\boldsymbol{J}_e] = \text{row-rank}[\boldsymbol{C}] = \text{column-rank}[\boldsymbol{F}]$$

then a weighted generalized inverse matrix can be obtained, which is defined to be

$$\boldsymbol{J}_e^{\#} = \boldsymbol{C}^T[\boldsymbol{C}\boldsymbol{C}^T]^{-1}\left[\boldsymbol{F}^T\boldsymbol{M}_x\boldsymbol{F}\right]^{-1}\boldsymbol{F}^T\boldsymbol{M}_x \tag{11}$$

With Eq. (11), the solution may be written as

$$\dot{\boldsymbol{d}} = \boldsymbol{J}_e^{\#}\dot{\boldsymbol{x}}_e + \left(\boldsymbol{I} - \boldsymbol{J}_e^{\#}\boldsymbol{J}_e\right)\dot{\boldsymbol{d}}_r' \tag{12}$$

which is just the solution of $\boldsymbol{M}_x$-least-squares error and minimum norm.

If $\boldsymbol{J}_e$ is of full rank (row-rank or column-rank), then its decomposition is trivial. In our case, $\boldsymbol{J}_e$ can be always considered to be of full row-rank. Thus, an obvious decomposition for $\boldsymbol{J}_e$ is to let $\boldsymbol{F} = \boldsymbol{I}$, where $\boldsymbol{I}$ is the identity matrix, such that $\boldsymbol{J}_e = \boldsymbol{C}$. Hence,

$$\boldsymbol{J}_e^{\#} = \boldsymbol{C}^T[\boldsymbol{C}\boldsymbol{C}^T]^{-1} = \boldsymbol{J}_e^T\left(\boldsymbol{J}_e\boldsymbol{J}_e^T\right)^{-1} = \boldsymbol{J}_e^{+}$$

which implies that $\boldsymbol{J}_e^{\#}$ is invariant to the choice of any matrix $\boldsymbol{M}_x$ so that the solution $\dot{\boldsymbol{d}}$ is independent of $\boldsymbol{M}_x$ and can be solved with Eq. (9). In fact, even if $\boldsymbol{J}_e$ is not of full row-rank, whenever vector $\boldsymbol{x}$ is in range$[\boldsymbol{J}_e]$, that is, $\boldsymbol{x} = \boldsymbol{J}_e\dot{\boldsymbol{d}}_1$ for some $\dot{\boldsymbol{d}}_1$ in $U$, then we can obtain

$$\boldsymbol{x}_s = \boldsymbol{J}_e^{\#}\boldsymbol{J}_e\dot{\boldsymbol{d}}_1 = \boldsymbol{C}^T[\boldsymbol{C}\boldsymbol{C}^T]^{-1}\left[\boldsymbol{F}^T\boldsymbol{M}_x\boldsymbol{F}\right]^{-1}\boldsymbol{F}^T\boldsymbol{M}_x\boldsymbol{F}\boldsymbol{C}\dot{\boldsymbol{d}}_1 = \boldsymbol{C}^{+}\boldsymbol{C}\dot{\boldsymbol{d}}_1$$

provided $\boldsymbol{J}_e$ has full-rank decomposition, $\boldsymbol{J}_e = \boldsymbol{F}\boldsymbol{C}$. This result gives rise to a useful conclusion, that is, the solution of a linear equation group $\dot{\boldsymbol{x}}_e = \boldsymbol{J}_e^{\#}\dot{\boldsymbol{d}}$ is invariant to the choice of matrix $\boldsymbol{M}_x$, if $\dot{\boldsymbol{x}}_e$ is in range$[\boldsymbol{J}_e]$, which is the most general case for a VGT considering

its highly redundant DOF. When $J_e$ is of full row-rank, the solution can be given directly using $J_e^T$. However, it must be stated that even though Eq. (9) is employed, the solution is implicitly relevant to the $M_x$-least-squares error and minimum norm.

*2. Inverse Kinematics of Motion Constraint*

According to the conclusion just drawn, Eq. (9) could be utilized to proceed with the following discussions. In general, an arbitrary vector $\dot{d}_r'$ might be used to meet some auxiliary optimal criterion, e.g., the work space of an end effector and so on. In addition, it can be employed to satisfy some secondary control goals. A typical case is obstacle avoidance. Concerning a free-floating VGT, its obstacle avoidance and shape control can always be achieved through handling the partial components of the center of mass velocities of a group of passive planes. Assume the passive planes group to be controlled is $P = \{p_{i_1}, p_{i_2}, \ldots, p_{i_m}\}$, where $p_{i_j}$ is the center of mass vector of a passive plane. By assigning a group of velocities $\dot{c}_j$, $j \in (1, \ldots, m)$ to them, a group of inverse kinematic equations similar to Eq. (5) can be established as motion constraints:

$$J_{i_j}\dot{d} = \dot{p}_{i_j} = \dot{c}_j \qquad j \in (1, \ldots, m) \tag{13}$$

where $J_{i_j}$ is the Jacobian matrix of a passive plane. Assembling all of these constraint equations into an integrated form, the inverse kinematics of motion constraints can be established:

$$J_c\dot{d} = \dot{c} \tag{14}$$

where $J_c$ is defined to be the Jacobian matrix of motion constraints.

Moreover, in case the free endplane needs to be partially controlled, the corresponding inverse kinematic equations can be constructed:

$$J_0\dot{d} = \dot{x}_0 \tag{15}$$

where $J_0$ is the Jacobian matrix for the free endplane, which can be obtained similarly to the Jacobian matrix in Eqs. (8–8c), and $\dot{x}_0$ is planned motion for the free endplane, including its orientation and, if needed, translation.

The lower control tasks such as shape control, obstacle avoidance, and free endplane control, etc., can be achieved with the corresponding inverse kinematics as motion constraints.

*3. Two-Order Inverse Kinematic Solution of Task Priority*

To deal with the mentioned motion constraints, vector $\dot{d}_r'$ can be utilized. However, these constraints commonly need to be divided into several control subtasks of priority. In the case where there are still enough DOF to guarantee the first-order constraint control, we can have the following formulation by simply substituting Eq. (9) into Eq. (14):

$$\dot{d} = J_e^+\dot{x}_e + J_1^+\dot{x}_1 + \left(I - J_e^+J_e\right)\left(I - J_1^+J_1\right)\dot{d}_{r_1}' \tag{16}$$

$$J_1 = J_{c_1}\left(I - J_e^+J_e\right) \quad \text{and} \quad \dot{x}_1 = \dot{c}_1 - J_{c_1}J_e^+\dot{x}_e \tag{16a}$$

Equation (16) can be further simplified using equation $B[CB]^+ = [CB]^+$, if $B$ is Hermitian and idempotent[7]; then

$$\dot{d} = J_e^+\dot{x}_e + J_1^+\dot{x}_1 + \left(I - J_e^+J_e - J_1^+J_1\right)\dot{d}_{r_1}' \tag{17}$$

The third term of Eq. (16) or (17) is defined as the intersection of both of $N(J_e)$ and $N(J_1)$. If the set of $N(J_e) \cap N(J_1)$ is nonempty, or of rank$[(I - J_e^+J_e)(I - J_1^+J_1)] > 0$, we could further obtain the second-order solution of Eq. (8), which is applied to a two-level control scheme of task priority:

$$\dot{d} = J_e^+\dot{x}_e + J_1^+\dot{x}_1 + J_2^+\dot{x}_2 + \left(I - J_e^+J_e - J_1^+J_1 - J_2^+J_2\right)\dot{d}_{r_2}' \tag{18}$$

$$J_2 = J_{c_2}\left(I - J_e^+J_e - J_1^+J_1\right) \quad \text{and} \quad \dot{x}_2 = \dot{c}_2 - J_{c_2}\left(J_e^+\dot{x}_e + J_1^+\dot{x}_1\right) \tag{18a}$$

Observing Eqs. (17) and (18), note the recurrence of the general solution of the $n$th-order task priority. However, a two-order solution is sufficient to fulfill the task requirements in our case, which is discussed in more detail.

### C. Several Applications for Two-Order Inverse Solution of Task Priority

*1. Docking Control with Obstacle Avoidance*

A typical docking problem might be that a free-floating VGT is constrained by environmental conditions, which can be abstracted into several obstacles, while one of its working endplanes is maneuvered to move toward to a docking target. Concerning these obstacles, the inverse kinematics of motion constraints can be established as in Eq. (14), where the Jacobian matrix of motion constraint takes the following form:

$$J_c = \left\{J_{r_1}, \ldots, J_{r_m}\right\}^T \tag{19}$$

where

$$J_{r_i} = \left\{T_{r_i}\left(-A_{r_i,0}H_0^{-1}H_1 + A_{r_i,1}\right), \ldots, T_{r_i}\left(-A_{r_i,0}H_0^{-1}H_N + A_{r_i,N}\right)\right\}$$

is the Jacobian matrix corresponding to the $r_i$th passive plane and $T_{r_i}$ is the transformation matrix used to eliminate some rows of Jacobian matrix that are not treated. The obstacle avoidance can be taken as the first-order control task. In addition, it is meaningful to take into account the control of the free endplane. In fact, the free-endplane cannot be completely free, in that the motion of the free endplane is certainly restricted by workspace limitations in most applications. Consequently, it has practical meaning to consider the case where the free endplane must be kept static to support some other body, etc., during the course of docking, which might be achieved by the second solution of Eq. (18).

*2. Simultaneously Docking with Two Endplanes of a Free-Floating VGT*

When a free-floating VGT is to be assembled onto other components with its two endplanes, a two-order solution given by Eq. (18) might suggest a feasible docking scheme, i.e., simultaneously docking with the two endplanes of the structure. This control scheme can be made possible if the two docked targets are exactly located in the workspaces of the two endplanes and the structure is equipped with enough actuators. Concerning this case, we would like to choose the first-order solution for maneuvering the 0th passive plane of the structure. Then, the second-order solution can be left, if needed, for avoiding obstacles. The Jacobian matrix for the other endplane can be represented in a form similar to Eq. (15).

*3. Autonomous Motion of a VGT with Two Fixed Endplanes*

While the two endplanes of the structure are kept static, and whereas some passive planes are made to move along with some specified velocity patterns, an autonomous motion of the structure can be achieved to alter the shape curve of the structure formed in space. If the velocity distribution pattern of each passive plane can be determined according to the particular task requirement, then the inverse kinematics of motion constraints can be established, as in Eq. (15). Since the more important control is for the two endplanes, where one is taken as the major control task and the other as the first-order control task, the self-motion of the structure can be described by the second-order solution expressed as

$$\dot{d} = J_{c_2}\left(I - J_e^+J_e - J_1^+J_1\right)\dot{c}_2 \tag{20}$$

where $J_1$ is given by Eq. (16a).

## IV. Analysis on the Singularities of Free-Floating VGTs

In the course of controlling a VGT with its inverse kinematics, the motion singularities may be a crucial problem. Concerning VGTs, singularities occur not only in the case that the Jacobian matrix of structures is singular, but also when actuators reach their mechanical limits so that some DOF are lost. The former can be discovered by determining the rank of the Jacobian matrix, and the latter can be avoided through checking workspaces. It is easy to observe that usually VGTs soon become singular when the rotation of the end effectors is actively controlled. As a matter of fact, a VGT bay (see Part 1) has limited motion ability and shows almost no rotation. For this reason, a control scheme is employed just to maneuver the

five DOF of the end effector of the VGT in this study. A VGT's singularities can be easily determined if it is fixed to some platform, in that in this case the singularities of a VGT are kinematic, occurring when at least three $\boldsymbol{d}$ vectors that correspond to three bays are in the same plane. In addition, singularities can be found when there are three angular velocities relevant to three bays in the same plane. However, these simple characteristics for predicting singularities are not available when considerating free-floating VGTs.

### A. Dynamic Singularity

In the case of free-floating space manipulators, it has been pointed out[8] that dynamically singular configurations exist, which are related to the dynamic properties of structural systems and cannot be predicted solely from the kinematic structure of VGTs. As to a free-floating VGT, it is easy to prove this point by observing [Eqs. (8–8c)] that the generalized Jacobian matrix of a free-floating VGT contains the contributions from inertial momentum and mass. Concerning this fact, several points can be made.

1) The singular points in the space of the control variable of free-floating VGTs change because of different dynamic properties of the system, which makes it very difficult to conclude singular configurations of free-floating VGTs in a broad scope, and so the motion planning of free-floating VGTs becomes a serious problem.

2) For the free-floating VGTs with the same kinematic structures, there exists no identical workspace for different dynamic parameters of structures, which brings about a serious difficulty in estimating the working abilities of VGTs.

3) Though singular points in the space of the control variable can be mapped into unique points in the workspace corresponding to particular dynamic properties, i.e., masses and inertia, it is shown by the experiment that these points in the workspace can be reached with other nonsingular configurations, which implies that the free-floating VGT singularities in the workspace are configuration dependent.

### B. Avoidance of Dynamic Singularity

Basically, the dynamic coupling of the singularities of a free-floating VGT arises from the mutual reaction of the two endplanes, which leads to the generalized Jacobian matrix, which is highly dependent on the dynamic properties of the system. Consequently, avoiding directly employing the generalized Jacobian matrix may be a way to reduce the effect of the dynamic singularities. To this end, let us rewrite Eq. (8):

$$\dot{\boldsymbol{x}}_e = \boldsymbol{J}_0\dot{\boldsymbol{\Phi}}_0 + \boldsymbol{J}_d\dot{\boldsymbol{d}} \tag{21}$$

$$\boldsymbol{J}_0 = \begin{Bmatrix} \boldsymbol{A}_{N,0} \\ \boldsymbol{N}_0 \end{Bmatrix} \quad \text{and} \quad \boldsymbol{J}_d = \begin{Bmatrix} \boldsymbol{A}_{N,1}, \ldots, \boldsymbol{A}_{N,N} \\ \boldsymbol{N}_1, \ldots, \boldsymbol{N}_N \end{Bmatrix} \tag{21a}$$

Usually, a VGT is highly redundant so that some DOF can be used to actively control $\dot{\boldsymbol{\Phi}}_0$ with a prespecified pattern. In this case, from Eq. (21) we obtain

$$\dot{\boldsymbol{d}} = \boldsymbol{J}_d^+\left(\dot{\boldsymbol{x}}_e - \boldsymbol{J}_0\dot{\boldsymbol{\Phi}}_0\right) + \left(\boldsymbol{I} - \boldsymbol{J}_d^+\boldsymbol{J}_d\right)\dot{\boldsymbol{d}}'_{r_1} \tag{22}$$

Substitute Eq. (22) into Eq. (3) to solve $\dot{\boldsymbol{d}}'_{r_1}$, and, finally, we arrive at

$$\dot{\boldsymbol{d}} = \dot{\boldsymbol{d}}_x - \left(\boldsymbol{I} - \boldsymbol{J}_d^+\boldsymbol{J}_d\right)\boldsymbol{J}_{hd}^+\left(\boldsymbol{H}_d\dot{\boldsymbol{d}}_x + \boldsymbol{H}_0\dot{\boldsymbol{\Phi}}_0\right) + \left(\boldsymbol{I} - \boldsymbol{J}_d^+\boldsymbol{J}_d\right)\left(\boldsymbol{I} - \boldsymbol{J}_{hd}^+\boldsymbol{J}_{hd}\right)\dot{\boldsymbol{d}}'_{r_2} \tag{23}$$

where $\dot{\boldsymbol{d}}_x = \boldsymbol{J}_d^+\left(\dot{\boldsymbol{x}}_e - \boldsymbol{J}_0\dot{\boldsymbol{\Phi}}_0\right)$ and $\boldsymbol{J}_{hd} = \boldsymbol{H}_d\left(\boldsymbol{I} - \boldsymbol{J}_d^+\boldsymbol{J}_d\right)$.

Observing Eq. (23), note that instead of the generalized Jacobian matrix, the Jacobian matrix $\boldsymbol{J}_d$ is employed to establish the two-order solution for free-floating VGTs. Commonly, the inertial matrix $\boldsymbol{H}_d$ is of full rank. Therefore, the singularities of the system rely only on the singular points of $\boldsymbol{J}_d$, which is independent from the rotational inertia of the system and is just relevant to the distribution of mass of the system. With the Jacobian matrix $\boldsymbol{J}_d$, the singular configurations of a free-floating VGT similar to its kinematic singularities can be obtained, which can then be defined to be the pseudokinematic singularities of the system.

Thus far, a point concerning dynamic singularities of a free-floating VGT can be made that by actively controlling the orientation of its free endplanes, the dynamic singularities can be qualitatively reduced such that the pseudokinematic singularities of systems can be obtained.

## V. Docking Experiment of a VGT

### A. Physical Model of a VGT

Figure 2 shows the dimensions of a VGT model with four bays. Each triangular batten has three actuators, which consist of ball screws and motors. The motors installed at even numbered battens or, in other words, active planes, possess encoders, and those at odd battens, namely, passive planes, have no encoders. Any motor without an encoder is not operated in this investigation. The whole model is suspended by five wires about 2 m in length from a straight rail fixed to the laboratory ceiling. The suspension points of the model are all odd-numbered planes, where the other endtips of the wires are fixed at five pulleys, the blocks of which are mounted on five horizontal spindles (Fig. 3). Such a suspension mechanism can allow the suspension points of the wires to move simultaneously along both the rail and spindles through the bearing attachment and rolling wheels of the pulleys, respectively, which could be used to roughly simulate a null-gravity state within two dimensional space if and only if the centers of mass of all planes, including both active and passive planes, are set within the same horizontal plane. Table 1

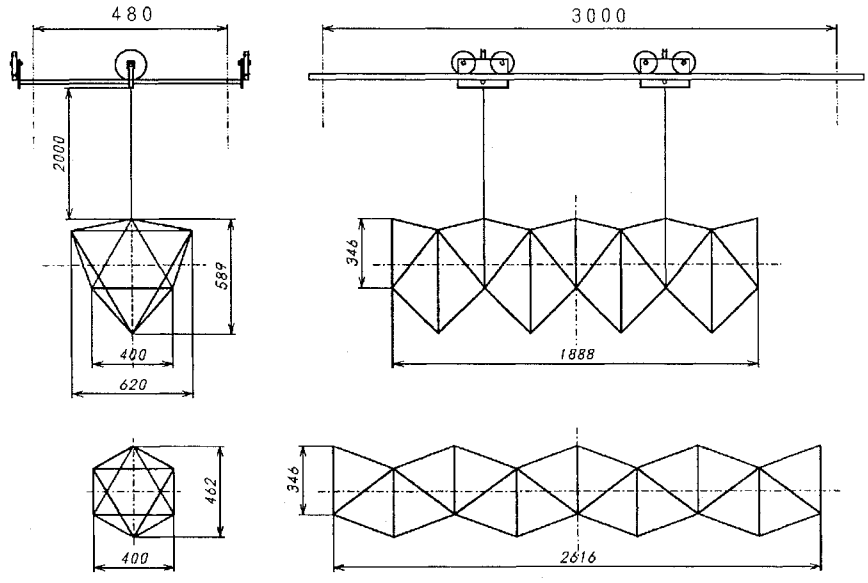


**Fig. 2 Dimension of a VGT model and its setup.**

**Table 1 Scale specification of each member**

| | Diameter, mm | Min. length, mm | Max. length, mm | Actuator stroke, mm |
|---|---|---|---|---|
| Actuator member with encoder | 18 | 400 | 651 | 220 |
| Actuator member without encoder | 18 | 400 | 651[a] | 220[a] |
| Diagonal member | 12 | 400 | | |

[a]Not used in this study.

**Table 2 Weight specification of components**

| | | |
|---|---|---|
| 1) Triangular member | Ball screw | 300 g |
| | Ball unit | 160 g |
| | Pipe unit | 70 g |
| 2) Actuator unit | With encoder (2 – 1) | 200 g |
| | Without encoder[a] (2 – 2) | 210 g |
| 3) Diagonal member | | 40 g |
| 4) Hinge | | 50 g |
| Total weight[b] | | 23.13 kg |

[a]With limiter. [b]That is, (1) × 27 + (2 – 1) × 12 + (2 – 2) × 15 + (3) × 48 + (4) × 27.

**Table 3 Specification of an actuator system**

| | | |
|---|---|---|
| dc servoactuator | Rated output power, W | 1.7 |
| | Rated torque, kg-cm | 3.0 |
| | Rated current, A | 0.5 |
| | Rated speed, rpm | 55 |
| | Weight, kg-cm | 0.07 |
| Encoder | Resolution, pulse/revolution | 100 |
| Gear system | Stepup rate | 1:3 |
| Ball screw | Pitch, mm | 0.4 |

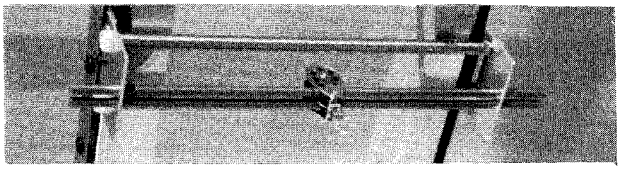

**Fig. 3 Suspension mechanism of a VGT model.**

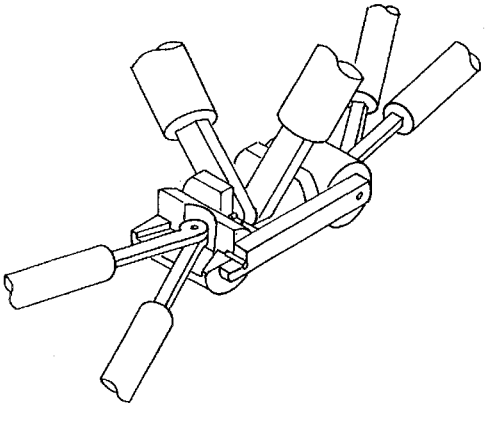

**Fig. 4 Hinge design.**

shows the scale of each member, and Table 2 gives the weight of each component.

A VGT consists of many octahedral truss elements and keeps good symmetrical characteristics, which allows for a simple design for its hinges. Figure 4 shows the hinge design of the model. The actual hinge of the model is shown in Fig. 5. A motor with an encoder is shown in Fig. 5a, and one without an encoder is shown in Fig. 5b. The gear system and a ball screw are also seen in the photographs. Table 3 lists the specifications of an actuator system.

### B. Distributed Control Architecture of a VGT Experimental Model

The motors with encoders are dc servocontrol modules equipped. These control modules are connected to processors, which are then controlled by a central computer. The setup of the control

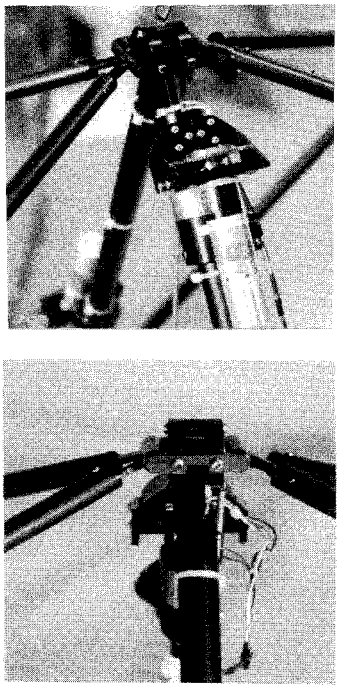

**Fig. 5 Hinge and actuator system.**

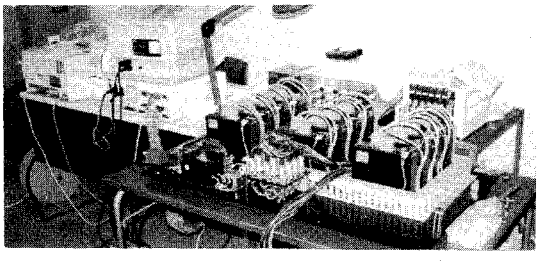

**Fig. 6 Setup of the control apparatus.**

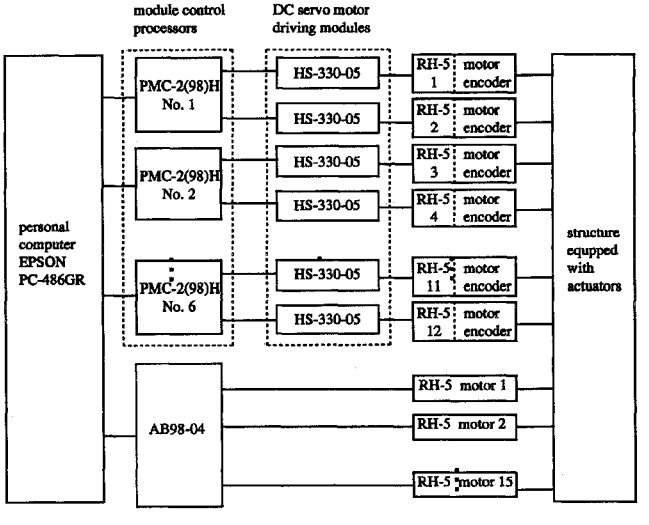


**Fig. 7 Control architecture of a VGT model.**

apparatus is shown in Fig. 6, and the control architecture of the VGT model is shown in Fig. 7. Obviously, this is distributed control architecture.

PMC-2(98)H is a control processor for pulse motor modules and can simultaneously handle two pulse motors through motor drive modules HS-330-05. It can drive a pulse motor to move at a constant speed to a prespecified position and speed up or slow down a pulse motor on demand; thus, it can provide the speed and position control. In addition, it receives and treats the feedback such as execution results, current state of the motor, manner of stopping, and

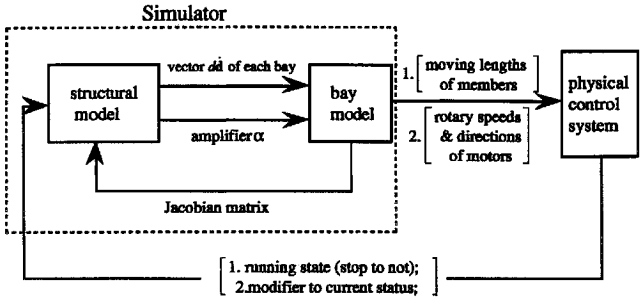


**Fig. 8 Implementation of control scheme.**

number of pulse left, from HS-330-05. HS-330-05 is a driving module for the dc servomotors. It decodes the inputs from PMC-2(98) and converts the decoded pulses to the motors. Moreover, it deals with the feedback from the encoders and sends out the messages of in position, overflow, and alarms, etc., to PMC-2(98)H.

### C. Control Scheme of a VGT Model

Figure 8 illustrates implementation of the control scheme of a VGT model. The overall control system is broken up into two mutually independent control blocks. One is responsible for the action response of the structure and the other, which is called the simulator, does computations for structural action of the next time step. These two control blocks are parallel in executing logic, which means the structural movement and digital simulation can be carried out simultaneously. Viewed from the time sequence of achievement of the control, the structural action response is delayed only a time step than a computation.

### D. Achievement of Control Scheme

*1. Control Variables of the Orientation of the Docking Plane*

The most common choices for representing the normal vector of a docking plane are Euler angles $\varphi$ and $\theta$. In our case, $\varphi$ and $\theta$ are defined to be the angles that rotate about axes $X$ and $Y$, respectively, where axes $X$ and $Y$ are located in the docking plane; axis $Z$ is set to coincide with the normal direction of the docking plane. Thus,

$$\boldsymbol{n}_e = \{\sin\theta, -\sin\varphi\cos\theta, \cos\varphi\cos\theta\} \tag{24}$$

$$\bar{\Phi} = \begin{bmatrix} 0 & -\dfrac{\cos\varphi}{\cos\theta} & \dfrac{\sin\varphi}{\cos\theta} \\ \cos\theta & \sin\varphi\sin\theta & -\cos\varphi\sin\theta \end{bmatrix} \tag{25}$$

*2. Control Approach*

Because the actuators equipped with a VGT model are limited in number, the docking experiment is carried out without considering obstacles and the free-endplane control. Concerning the specification of trajectory for the docking plane, the treatment is to keep the velocity direction of the center of mass of the docking plane always oriented to the center of mass of the docking port. The overall docking procedure is divided into two stages. The first is a moving process handled considering environmental conditions rather than the inverse kinematics, after which the docking plane enters the vicinity of the docking port. Then the docking is accomplished under inverse kinematic control.

*3. Knowledge Base of Control*

Building a knowledge base of control is a key to supporting intelligent VGTs. In this study, the knowledge base of control is established on the abstraction of object-oriented concepts.[9] With an object-oriented model, a two-level control architecture is modeled. The first level is for the distributed actuator system, which includes servomotors, driving modules, and control processors. The second level is responsible for the synergy of the behavior of all bays through motion planning. With a simple communication system between the central computer and processors, parallel control is achieved. To date, the control flow achieved is still one way, starting from the considering docking requirements, adjusting structural motion, and finally determining actuator responses. However, based on the object-oriented model for free-floating VGTs, a control scheme based on the autonomous behaviors of each bay may be made available in the future.

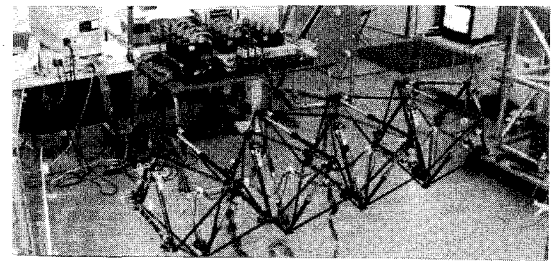

**Fig. 9 Initial state of the VGT model.**

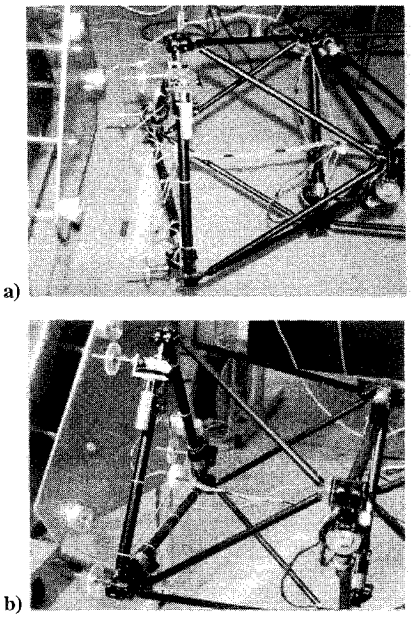


**Fig. 10 Two moving states of the VGT model.**

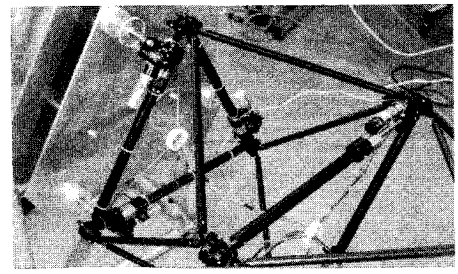

**Fig. 11 Finishing state of the VGT model.**

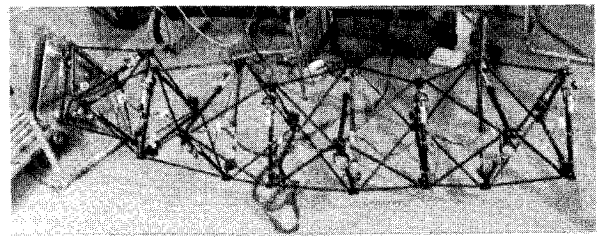

**Fig. 12 Final shape of the VGT model after docking.**

### E. Experimental Process of VGT Model

Figure 9 shows the initial state of the experimental VGT model, Figs. 10a–11 roughly show the process of structural docking at three stages. Figure 12 then shows the final shape formed by the VGT after accomplishing the docking to the target.

## VI. Discussion of the Experimental Results

Through the experiment, we found that the workspace of the two endplanes of a free-floating VGT cannot form an ellipsoid formed by two-dimensional free-floating link structures.[3] In fact, just some boundary points of the ellipsoid are accessible. Moreover, these accessible points are tightly bound up with specific configurations of a free-floating VGT, which implies that the free-floating VGT will experience strong singularities in the course of moving toward the docking target. Obviously, this is because of the effects of the dynamic singularities. Hence, keeping better configurations for free-floating VGTs is a key to extending their workspaces. Concerning this problem, the Moore–Penrose inverse kinematic solutions have severe drawbacks when they are applied to the control of free-floating VGTs. Note that the Moore–Penrose inverse always makes a free-floating VGT form an even-order curve because of its features of minimum norm and least squares, whereas we found in the experiment that lower odd-order curves of a free-floating VGT provide more extensive workspaces. Except the major docking tasks, especially whenever avoidance of an obstacle or control of a free-endplane is included as a secondary task, a higher even-order curve formed by a free-floating VGT is always caused, so that workspaces are greatly limited.

Consequently, we cannot help considering that it is unnecessary to make the docking endplane always move along some precisely defined trajectory, except during the final docking treatment. In fact, more important for VGTs than their docking control is their shape control. However, no straightforward way is provided for the inverse kinematic control to manipulate the shape of free-floating VGTs. Further investigations are in progress.

## VII. Conclusion

The report presented here is a continuation of the investigations about the motion control of free-floating variable geometry trusses, dealing with the aspects of including the inverse kinematics for docking control, the construction of control architecture for a variable geometry model in the laboratory, as well as the corresponding experiment. In this paper, the inverse kinematics equations of free-floating VGTs are derived, and the solving approaches using the Moore–Penrose inverse are discussed. The dynamic singularities of a free-floating VGT are discussed, and a method to reduce their dynamic coupling is proposed through actively handling the orientation of the free endplane. Concerning the applications of the Moore–Penrose inverse, the dimensional inhomogeneity of the inverse kinematic solutions is touched on with regard to the physically inconsistent end-effector control variables, and a two-order solution of task priority is presented. With a two-order solution of task priority, several control schemes are suggested, and the corresponding applications are described. In addition, a VGT model is introduced in detail, including its hinge design, distributed control architecture, and setup in the laboratory. Finally, the docking experiment process with this model is shown using photographs.

## Acknowledgment

The authors wish to express their appreciation to Masamori Sakamaki at the Institute of Space and Astronautical Science for his helpful work on enhancing the control ability of the VGT model.

## References

[1]Huang, S., Natori, M. C., and Miura, K., "Motion Control of Free-Floating Variable Geometry Truss Part 1: Kinematics," *Journal of Guidance, Control, and Dynamics*, Vol. 19, No. 4, 1996, pp. 756–763.

[2]Umetani, Y., and Yoshida, K., "Resolved Motion Rate Control of Space Manipulators with Generalized Jacobian Matrix," *IEEE Transactions on Robotics and Automation*, Vol. 5, No. 3, 1989, pp. 303–314.

[3]Miura, K., and Matunaga, S., "An Attempt to Introduce Intelligence in Structures," *Proceedings of the AIAA/ASME/ASCE/AHS/ASC 35th Structures, Structural Dynamics, and Materials Conference* (Mobile, AL), AIAA, Washington, DC, 1989, pp. 1145–1153 (AIAA Paper 89-1289).

[4]Liegeois, A., "Automatic Supervisor Control of the Configuration and Behavior of Multibody Mechanisms," *IEEE Transactions on Systems, Man, and Cybernetics*, Vol. SMC-7, No. 12, 1977, pp. 868–871.

[5]Doty, K. L., et al., "A Theory of Generalized Inverse Applied to Robotics," *International Journal of Robotics Research*, Vol. 12, No. 1, 1993, pp. 1–19.

[6]Ben-Israel, A., and Greville, T. N. E., *Generalized Inverse: Theory and Applications*, Wiley, New York, 1974.

[7]Maciejewski, A. A., and Klein, C. A., "Obstacle Avoidance for Kinematically Redundant Manipulators in Dynamically Varying Environments," *International Journal of Robotics Research*, Vol. 4, No. 3, 1985, pp. 109–117.

[8]Papadopoulos, E., and Dubowsky, S., "On the Dynamic Singularities in the Control of Free-Floating Space Manipulators," *Dynamics and Control of Multibody/Robotic Systems with Space Applications*, edited by S. M. Joshi, L. Silverberg, and T. E. Alberts, ASME DSC-Vol. 15, American Society of Mechanical Engineers, New York, 1990, pp. 45–52.

[9]Huang, S. Y., Natori, M. C., Nakai, S., and Katukura, H., "An Object-Oriented Approach to the Motion Control of a Free-Floating Variable Geometry Truss," *Proceedings of the AIAA/ASME/ASCE/AHS/ASC 35th Structures, Structural Dynamics, and Materials Conference and the AIAA/ASME Adaptive Structures Forum*, AIAA, Washington, DC, 1994, pp. 465–473.